# REGIMES OF HARMONICALLY FORCED LINEAR OSCILLATOR WITH ATTACHED NONLINEAR ENERGY SINK NEAR THE MAIN RESONANCE

Yuli Starosvetsky
Faculty of Mechanical Engineering
Technion – Israel Institute of Technology
Technion City, Haifa, 32000, Israel
staryuli@tx.technion.ac.il

Oleg Gendelman[+]
Faculty of Mechanical Engineering
Technion – Israel Institute of Technology
Technion City, Haifa, 32000, Israel
ovgend@tx.technion.ac.il

**Abstract**

Dynamic responses of a linear oscillator coupled to a nonlinear energy sink (NES) under harmonic forcing in the regime of 1:1 resonance are investigated. Primary attention is paid to detailed investigation of so-called strongly modulated response (SMR), which is not related to the fixed points of average modulation equations of the system. It is demonstrated that the SMR is related to a relaxation – type motion and its description may be reduced to one – dimensional discrete mapping of a subset at a fold line of slow invariant manifold of the system.

## 1 Introduction

Recently it has been demonstrated that various systems comprised of linear substructures and strongly nonlinear attachments exhibit localization and irreversible transient transfer (pumping) of energy to prescribed fragments of structure dependent on initial conditions and external forcing [Gendelman O.V. (2001); Gendelman O.V., Vakakis A.F., Manevitch L.I. and McCloskey R., (2001); Vakakis A.F. and Gendelman O.V. (2001); Vakakis A.F. (2001)]. Addition of a relatively small and spatially localized attachment leads to essential changes in the properties of the whole system. Unlike common linear and weakly nonlinear systems, systems with strongly nonlinear elements are able to react efficiently on the amplitude characteristics of the external forcing in a wide range of frequencies [Vakakis A.F., Manevitch L.I., Gendelman O., Bergman L. (2003)]. Thus, the systems under consideration give rise to a new concept of nonlinear energy sink (NES).

In papers [Gendelman O.V., Starosvetsky Y. (2006); O.V. Gendeman, Y.Starosvetsky, M. Feldman (2007); Y.Starosvetsky , O.V. Gendelman (2007)] it was established that combination of essential nonlinearity and strong mass asymmetry brings about a possibility of response regimes qualitatively different from steady – state and weakly modulated responses existing in the vicinities of fixed points of averaged flow equations in conditions of 1:1 resonance. Thus, they cannot be described with the help of local analysis of the averaged flow equations.

The goal of present paper is to develop the analytic approach allowing one to describe frequency dependence and global bifurcations of the regime of SMR. Appropriate analytic and numeric tools are presented in Sections 2 and 3. Comparisons with direct numeric simulations of averaged and full flow are presented in Section 4, followed by concluding remarks in Section 5.

## 2 Description of the model and necessary conditions for the regime of SMR

The system under consideration is described by the following equations:

$$\ddot{y}_1+\varepsilon\lambda(\dot{y}_1-\dot{y}_2)+(1+\varepsilon\sigma)y_1+ +\frac{4}{3}\varepsilon(y_1-y_2)^3=\varepsilon A\cos t$$

$$\varepsilon\ddot{y}_2+\varepsilon\lambda(\dot{y}_2-\dot{y}_1)+\frac{4}{3}\varepsilon(y_2-y_1)^3=0 \quad (1)$$

where $y_1$ and $y_2$ are the displacements of the linear oscillator and the attachment respectively, $\varepsilon\lambda$ is the damping coefficient, $\varepsilon A$ is the amplitude of external force and $\varepsilon\sigma$ is the frequency detuning parameter. $\varepsilon<<1$ is a small parameter which establishes the order of magnitude for coupling, damping, amplitude of the external force, detuning and mass of the attachment.

Coefficients: $A,\lambda,\sigma$ are adopted to be of order unity. Rigidity of the nonlinear spring is adopted to be equal to $\frac{4}{3}\varepsilon$ and linear frequency of the primary oscillator – close to unity.

Successive changes of variables provide:

$$v=y_1+\varepsilon y_2 \;\;;\;\; w=y_1-y_2$$
$$\varphi_1\exp(it)=\dot{v}+iv \;;\; \varphi_2\exp(it)=\dot{w}+iw \quad (2)$$

Substitution of new variables and averaging over one forcing period, yields:

$$\dot{\varphi}_1+\frac{i\varepsilon}{2(1+\varepsilon)}(\varphi_1-\varphi_2)-\frac{i\varepsilon\sigma(\varphi_1+\varepsilon\varphi_2)}{2(1+\varepsilon)}=\frac{\varepsilon A}{2}$$
$$\dot{\varphi}_2+\lambda(1+\varepsilon)\frac{\varphi_2}{2}+\frac{i}{2(1+\varepsilon)}(\varphi_2-\varphi_1)- -\frac{i\varepsilon\sigma(\varphi_1+\varepsilon\varphi_2)}{2(1+\varepsilon)}-\frac{i(1+\varepsilon)}{2}|\varphi_2|^2\varphi_2=\frac{\varepsilon A}{2} \quad (3)$$

Fixed points of Equations (3) correspond to periodic responses of the system described by Equation (1). By simple algebraic manipulations fixed points of (3) are obtained from:

$$\varphi_{10}=|\varphi_{10}|\exp(i\theta_{10})\;,\;\varphi_{20}=|\varphi_{20}|\exp(i\theta_{20})$$
$$\left[\lambda^2+\frac{\sigma^2}{(1-\sigma)^2}\right]|\varphi_{20}|^2+\frac{2\sigma}{1-\sigma}|\varphi_{20}|^4+|\varphi_{20}|^6=\frac{A^2}{(1-\sigma)^2};$$
$$\theta_{20}=\tan^{-1}\left(\frac{\sigma}{\lambda(1-\sigma)}+\frac{|\varphi_{20}|^2}{\lambda}\right)\;;\;|\varphi_{10}|=\frac{1+\varepsilon\sigma}{1-\sigma}\frac{|\varphi_{20}|\cos\theta_{20}}{\cos\theta_{10}}$$
$$\theta_{10}=\tan^{-1}\left(\tan\theta_{20}-\frac{(1+\varepsilon)A}{(1+\varepsilon\sigma)|\varphi_{20}|\cos\theta_{20}}\right) \quad (4)$$

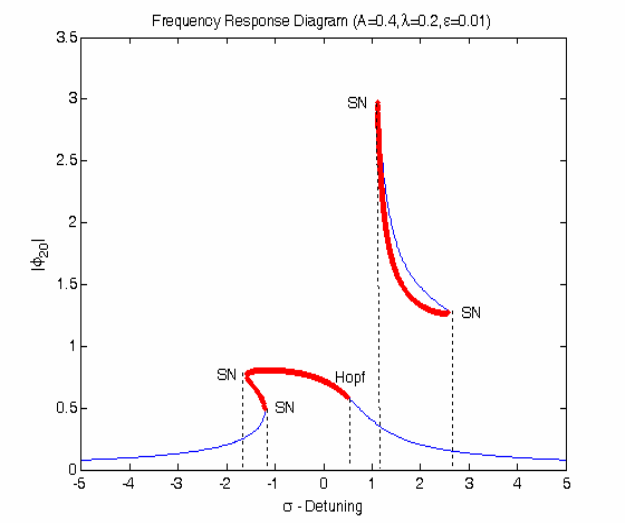


Figure 1. Bold red lines refer to the unstable regions of the periodic solutions when the thin lines refer to the stable regions

System (4) has somewhat special form - the time derivative in the first equation is proportional to the small parameter and thus the time evolution of variable $\varphi_1$ can be considered as slow compared to $\varphi_2$. This peculiarity means that the dynamics of System (4) in 4-dimensional real state space may be presented in terms of 2 "fast" and 2"slow" real variables, thus giving a chance of tractable global description.

By simple manipulations, System (3) may be reduced to single second – order ODE:

$$\frac{d^2\varphi_2}{dt^2}+\frac{d}{dt}\left[\alpha\varphi_2-\frac{i(1+\varepsilon)}{2}|\varphi_2|^2\varphi_2+\frac{i\varepsilon}{2(1+\varepsilon)}(1-\sigma)\varphi_2\right]+ +\frac{i\varepsilon}{2(1+\varepsilon)}(1-\sigma)\left[\alpha\varphi_2-\frac{i(1+\varepsilon)}{2}|\varphi_2|^2\varphi_2-\frac{\varepsilon A}{2}\right]- -\frac{i\varepsilon\beta}{2(1+\varepsilon)}[1+\varepsilon\sigma]\varphi_2=\frac{\varepsilon A\beta}{2}$$

$$\alpha = \frac{\lambda(1+\varepsilon)^2 + i - i\varepsilon^2\sigma}{2(1+\varepsilon)} \; ; \; \beta = \frac{i}{2(1+\varepsilon)}(1+\varepsilon\sigma) \tag{5}$$

Multiple scale expansion is introduced as:

$$\varphi_2 = \varphi_2(\tau_0, \tau_1, ...) \; ; \; \frac{d}{dt} = \frac{\partial}{\partial \tau_0} + \varepsilon \frac{\partial}{\partial \tau_1} + ...$$

$$\tau_k = \varepsilon^k t, k = 0,1,... \tag{6}$$

Substituting (6) into (5) and equating the like powers of $\varepsilon$ one obtains equations for zero and the first order approximations::

$$\varepsilon^0 : \; \frac{\partial^2 \varphi_2}{\partial \tau_0^{\,2}} + \frac{\partial}{\partial \tau_0}\left[\frac{\lambda\varphi_2}{2} + \frac{i\varphi_2}{2} - \frac{i}{2}|\varphi_2|^2 \varphi_2\right] = 0$$

$$\varepsilon^1 : \; 2\frac{\partial^2 \varphi_2}{\partial \tau_0 \partial \tau_1} + \frac{\partial}{\partial \tau_1}\left[\frac{\lambda\varphi_2}{2} + \frac{i\varphi_2}{2} - \frac{i}{2}|\varphi_2|^2 \varphi_2\right] +$$

$$+ \frac{\partial}{\partial \tau_0}\left[\frac{\lambda\varphi_2}{2} + \frac{i(1-\sigma)\varphi_2}{2} - \frac{i}{2}|\varphi_2|^2 \varphi_2\right] +$$

$$+ \frac{1-\sigma}{4}|\varphi_2|^2 \varphi_2 + \left[\frac{\sigma}{4} + \frac{i\lambda(1-\sigma)}{4}\right]\varphi_2 - \frac{iA}{4} = 0 \tag{7}$$

The first equation of (7) describes "fast" evolution of the averaged system. It can be trivially integrated:

$$\frac{\partial}{\partial \tau_0}\varphi_2 + (\frac{i}{2}\varphi_2 + \frac{\lambda}{2}\varphi_2 - \frac{i}{2}|\varphi_2|^2 \varphi_2) = C(\tau_1, ...) \tag{8}$$

where C is arbitrary function of higher – order time scales. Approximations of higher orders are not used in current analysis. Then for the sake of brevity only dependence on time scales $\tau_0$ and $\tau_1$ will be denoted explicitly below. Fixed points $\Phi(\tau_1)$ of Equation (8) depend only on time scale $\tau_1$ and obey algebraic equation:

$$\frac{i}{2}\Phi + \frac{\lambda}{2}\Phi - \frac{i}{2}|\Phi|^2 \Phi = C(\tau_1) \tag{9}$$

Equation (9) is easily solved by taking $\Phi(\tau_1) = N(\tau_1)\exp(i\theta(\tau_1))$ and performing trivial calculations:

$$\lambda^2 Z(\tau_1) + Z(\tau_1)(1 - Z(\tau_1))^2 = 4|C(\tau_1)|^2$$

$$Z(\tau_1) = (N(\tau_1))^2 \tag{10}$$

Figure 2 demonstrates projection of the two – dimensional SIM on the plane (N, C), the fold lines correspond to the points of maximum and minimum.

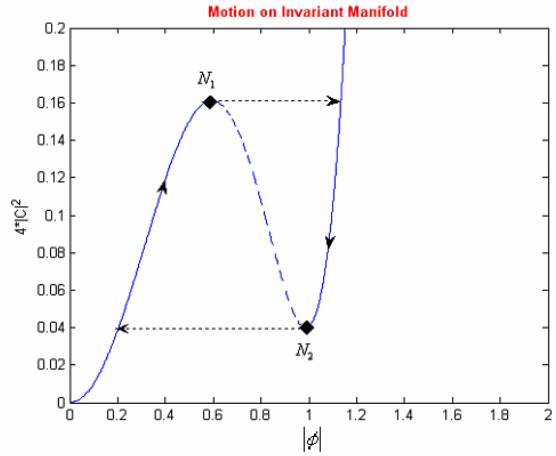


Figure 2 Projection of the slow invariant manifold of the system in accordance with Equation (10), λ=0.2

It is well-known [Arnold V I, Afrajmovich V S, Il'yashenko Yu S and Shil'nikov L P (1994); J. Guckenheimer, M. Wechselberger and Lai-Sang Young (2006); Guckenheimer J., Hoffman, K and Weckesser, W. (2005)] that such structure of the SIM may give rise to relaxation-type oscillations of the system. Still, such motion is possible only if the system can reach the fold lines while moving on the SIM with respect to the slow time scale. In order to assess this possibility, one should investigate the behavior of $\Phi(\tau_1)$. For this sake, we consider the $\varepsilon^1$ term of multiple – scale expansion namely the second equation of (7). We are interested in the behavior of the solution on the stable branches of the SIM $\Phi(\tau_1) = \lim_{\tau_0 \to +\infty} \varphi_2(\tau_0, \tau_1)$ . Taking the limit $\tau_0 \to \infty$ in the second equation of System (7) and taking into account the asymptotic stability of the points of the stable branches with respect to time scale $\tau_0$, one obtains:

$$\left[\frac{\lambda}{2} - \frac{i}{2} + i|\Phi|^2\right]\frac{\partial \Phi}{\partial \tau_1} - \frac{i}{2}\Phi^2 \frac{\partial \Phi}{\partial \tau_1} = G$$

$$G = -\frac{1-\sigma}{4}|\Phi|^2 \Phi - \left[\frac{\sigma}{4} + \frac{i\lambda(1-\sigma)}{4}\right]\Phi + \frac{iA}{4} \tag{13}$$

By taking complex conjugate of (13), it is possible to extract the derivative $\frac{\partial \Phi}{\partial \tau_1}$:

$$\frac{\partial \Phi}{\partial \tau_1} = \frac{2\left[\left(\lambda - i + 2i|\Phi|^2\right)G + i\Phi^2 G^*\right]}{\lambda^2 + 1 - 4|\Phi|^2 + 3|\Phi|^4} \qquad (14)$$

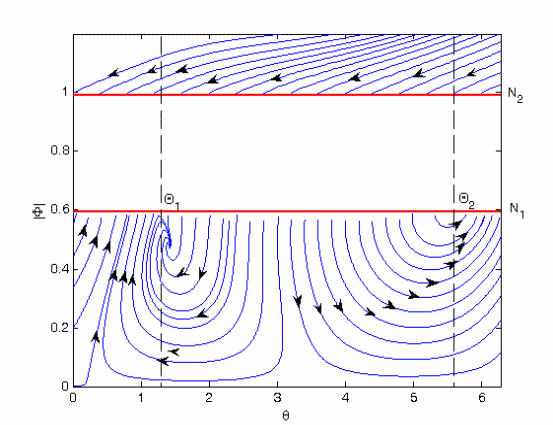


Figure 3. Phase portrait of the slow invariant manifold

### 3 Relaxation oscillations described by one – dimensional mapping

Observing the phase portrait presented at Fig. 3 we can see that there is an interval of $\theta$ - $[\Theta_1 < \theta < \Theta_2]$ for which all the phase trajectories are repelled from the lower fold $N_1$ ($|\Phi| = N_1$). In the regime of the relaxation oscillations, the phase trajectory jumps from a point of this interval to the upper branch of the SIM, then it moves along the line of the slow flow to the upper fold line, then jumps back to the lower branch and moves to the lower fold line, commencing in one of the points of the interval $[\Theta_1, \Theta_2]$ in order to enable the next jump. Therefore it is natural to consider this regime as mapping of the interval $[\Theta_1, \Theta_2]$ into itself – the regime of the relaxation oscillations will correspond to attractor of this one – dimensional map. Existence of this attractor is therefore necessary and sufficient condition for existence of the SMR for system (4), or, equivalently, equation (5), when the mass ratio ε is small enough.

In order to build the relevant mapping, we should consider separately the "slow" and the "fast" parts of the mapping cycle. As for the "slow" parts on the lower and the upper branches of the SIM, we can use equations (14) and directly connect the "entrance" and "exit" points. Due to complexity of the equations, this part of the mapping should be accomplished numerically. As for the "fast" parts, the function $\varphi_2$ should be continuous at the points of contact between the "fast" and the "slow" parts. Therefore, for "fast" parts of the motion one obtains complex invariant $C(\tau_1)$, defined by Equation (9). If one knows its value at the point of "start", it is possible co compute N and θ for the point of "finish" unambiguously and thus to complete the mapping. The procedure of numerical integration should be performed twice – for two branches of the SIM. Two invariants should be computed for two "fast" jumps, in order to determine their final points.

Not every trajectory which starts from the lower fold of the SIM will reach the initial interval since it may be attracted to alternative attractor at the upper or the lower branch of the SIM, if it exists. Of course, only those points which are mapped into the interval can carry sustained relaxation oscillations. The mapping procedure is illustrated at Figs. 4-5

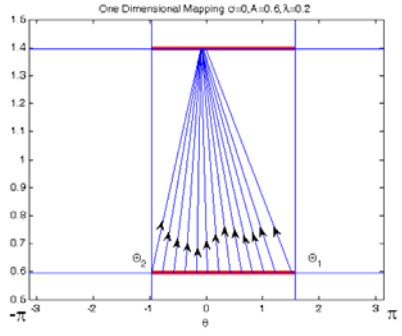


Figure 4 One dimensional mapping; $\sigma = 1, A = 0.6, \lambda = 0.2$.

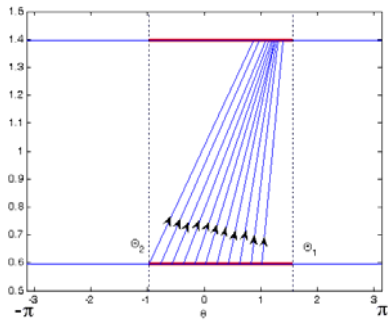

Figure 5 One dimensional mapping; $\sigma = 2.9, A = 0.6, \lambda = 0.2$.

. The mapping at Fig. 4 exists for all points of the interval and is obviously contractive, therefore one can expect existence of stable attractor corresponding to the regime of the relaxation oscillations (or SMR). By increasing the detuning parameter value (Fig. 5) one can notice that the mapping lines tend to the right and there is also a region on the basin which doesn't contain any lines. This region relates to the unaccomplished cycles, namely to the phase trajectories which started from the region and have been attracted to the periodic response attractor before they have reached the basin one more time. The mentioned trajectories are not illustrated on the diagram. It is clear from Fig. 6 that there is no stable attractor of the SMR and for every initial condition on the basin the system finally (after sufficient number of cycles) leaves the basin.

By now we can conclude that for some increased values of detuning parameter the SMR attractor vanishes.

Running with the values of detuning ($\sigma$) and for each step performing the mapping one can track the value of $\sigma$ for which the attractor vanishes. This provides a general tool for determination of the frequency region for the existence of strongly modulated response. For current system, the boundaries of the detuning parameter within which the SMR exists are $\sigma_R = 2.69 > \sigma > \sigma_L = -2.0546;$. So, as it was established earlier by direct numerical simulation, the SMR exists in rather small vicinity of the exact 1:1 resonance.

Our next goal is to investigate the mechanism of "birth" of the limit cycle related to the SMR when the detuning parameter passes its critical value. At Fig. 6 a sequence of mapping diagrams close to upper critical value of the detuning parameter ($\sigma = \sigma_R$) is presented.

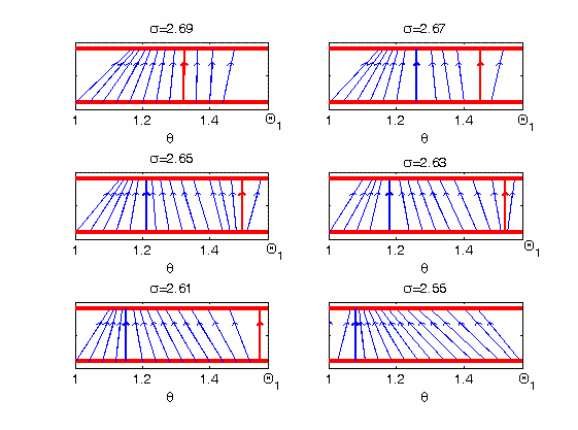


Figure 6 Sequence of mapping diagrams in the region ($1 < \theta < \Theta_1$); Horizontal bold lines refer to the basin of jump. Stable cycle marked with bold blue solid line and unstable is marked with the bold red solid line

For the boundary value ($\sigma = \sigma_R = 2.69$) we can see undistinguishable stable and unstable cycles, separating while the detuning parameter is decreased. This scenario corresponds to simple fold bifurcation of 1D map – creation of stable and unstable fixed points. It is essential also to check what happens about the left boundary ($\sigma_L$). In order to understand the mechanism by which the loss of the stable cycle occurs we have zoomed the area near the left end of the basin and plotted the diagrams for gradually decreasing values of $\sigma$ near the left boundary ($\sigma_L$) (Fig. 7).

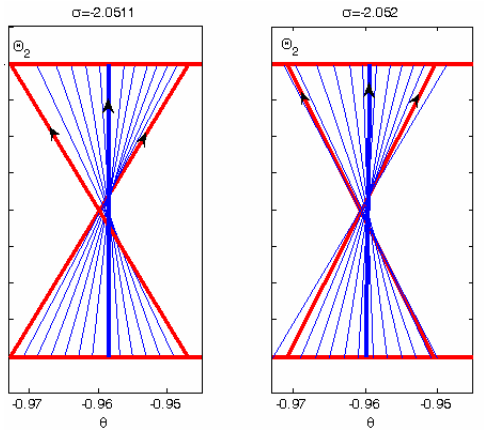


Figure 7 One dimensional mapping diagrams for $(\sigma = -2.0511, \sigma = -2.052)$. The bold red lines refer to the unstable double period cycle. The bold blue line refers to the stable one period cycle.

As one can see from the diagrams of Fig. 8 that for some value of detuning parameter we obtain the creation of the unstable double period cycle right on the left end of the basin. Slightly decreasing the detuning parameter value we can see the movement of the double period cycle from the left end of the basin inside the interior region.

The behavior of the SMR is described by 1D nonlinear map. Consequently, generic bifurcations of the 1D maps are expected to be observed also for these limit cycles in 4D state space. One of such generic bifurcations is period doubling, which exists for certain values of parameters. For example, picking a set of system parameters $A = 1, \lambda = 0.05, \sigma = 0$ one obtains the double period cycle of the one dimensional mapping (Fig. 11).

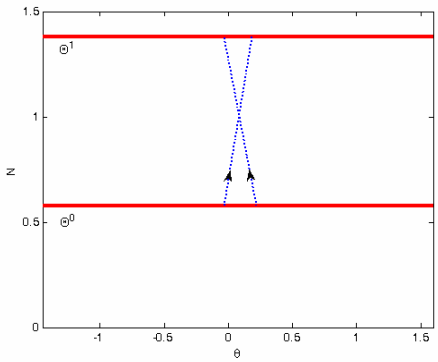


Figure 8 Double period cycle of the one dimensional mapping.

Additional period doubling bifurcations (e.g. from double period to for period cycle) were not observed in the mappings, however the period doublings are rater ubiquitous

It should be mentioned that the analytic approach developed above is valid in the limit $\varepsilon \to 0$. The approximation for finite values of $\varepsilon$ requires computation of the higher – order expansions for equation (7) and is rather cumbersome task. In this paper, we restrict ourselves by comparison of the analytic predictions with numeric simulations of original system (1) and averaged system (4).

Obtained analytical prediction of the SMR existence is in agreement with numerical simulation.

**4 Numeric simulations and verification of the analytic approach**

Our next goal is to verify numerically an analytical prediction of the SMR attractor existence described in the previous section. At Fig. 9 the analytic prediction obtained with the help of the one – dimensional mapping is compared to the numeric solutions of averaged system (4) for various initial conditions.

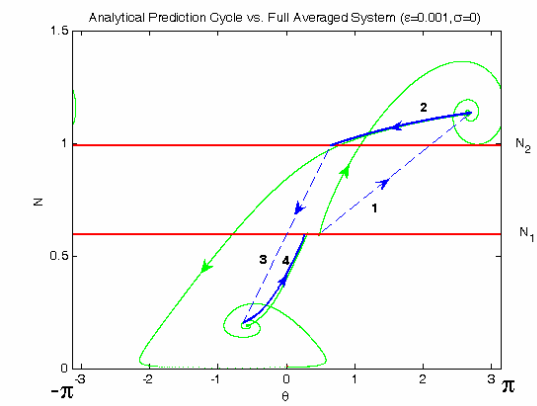


Figure 9 Blue arrowed lines refer to analytic predictions, green arrowed lines refer to numeric solution of averaged system (4) $\varepsilon = 0.001$ , $\sigma$=0

Then, we compare the numeric solution of the original system (1) with initial conditions

constrained to the SIM (with the same parameters as used for the plot of Fig. 4), with the analytic predictions.

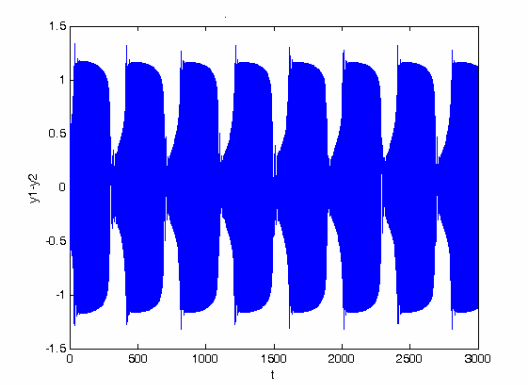


Figure 10 Time series for the SMR response

The frequency detuning interval obtained for the analytically predicted existence of the SMR attractor is [-0.9,1] when numerical simulation provides for $\varepsilon = 0.01$ - [-0.9, 0.9]. It is essential to note that the accuracy of the analytical prediction is increased with an epsilon reduction.

**5 Concluding Remarks**

The results presented in the above sections demonstrate that the SMR may be rather ubiquitous in the forced systems with essential nonlinearity and strong mass asymmetry. This type of response exists in a vicinity of exact 1:1 resonance and is characterized by relaxation oscillations between stable branches of the slow invariant manifold. Singular asymptotic procedure based on strong mass asymmetry allows reduction of the problem of describing the SMR to the one – dimensional nonlinear mapping of the subset of fold line on the SIM. It is therefore possible to study bifurcations of the global flow which bring about the creation or destruction of the SMR. Other generic bifurcations of 1D maps, like period doubling, also can be found in the system.

**References**


Gendelman O.V. (2001) Transition of Energy to Nonlinear Localized Mode in Highly Asymmetric System of Nonlinear Oscillators, *Nonlinear Dynamics*, **25**, 237-253.

Gendelman O.V., Vakakis A.F., Manevitch L.I. and McCloskey R., (2001) Energy Pumping in Nonlinear Mechanical Oscillators I: Dynamics of the Underlying Hamiltonian System, *Journal of Applied Mechanics*, **68**, n.1, 34-41.

Vakakis A.F. and Gendelman O.V. (2001) Energy Pumping in Nonlinear Mechanical Oscillators II: Resonance Capture, *Journal of Applied Mechanics*, **68**, n.1, 42-48.

Vakakis A.F. (2001) Inducing passive nonlinear energy sinks in linear vibrating systems Journal *of Vibration and Acoustics* **123**(3), 324-332.

Vakakis A.F., Manevitch L.I., Gendelman O., Bergman L. (2003) Dynamics of Linear Discrete Systems Connected to Local Essentially Nonlinear Attachments. *Journal of Sound and Vibration*, **264**, 559-577

Gendelman O.V., Starosvetsky Y. (2006) Quasiperiodic Response Regimes of Linear Oscillator Coupled to Nonlinear Energy Sink Under Periodic Forcing, in press, *Journal of Applied Mechanics*

O.V. Gendeman, Y.Starosvetsky, M. Feldman (2007) Attractors of Harmonically Forced Linear Oscillator with Attached Nonlinear Energy Sink I: Description of Response Regimes, in press, *Nonlinear Dynamics*

Y.Starosvetsky , O.V. Gendelman (2007), Attractors of Harmonically Forced Linear Oscillator with Attached Nonlinear Energy Sink II: Optimization of a Nonlinear Vibration Absorber , in press,, *Nonlinear Dynamics*

Arnold V I, Afrajmovich V S, Il'yashenko Yu S and Shil'nikov L P (1994) *Dynamical Systems V. Encyclopedia of Mathematical Sciences* (Berlin: Springer)

J. Guckenheimer, M. Wechselberger and Lai-Sang Young (2006), Chaotic attractors of relaxation oscillators, *Nonlinearity*, **19**, 701-720

Guckenheimer J., Hoffman, K and Weckesser, W. (2005), Bifurcations of Relaxation Oscillations near Folded Saddles,

*International Journal of Bifurcations and Chaos,* **15** (11), 3411-3421